Temperature-dependent nonlinear phonon behavior in high-density carbon nanotube thin films

A. Duzynska, J. Judek, and M. Zdrojek[a)]
Faculty of Physics, Warsaw University of Technology, Koszykowa 75, 00-662 Warsaw, Poland

(Received 7 October 2014; accepted 13 November 2014; published online 25 November 2014)

We report the temperature-dependent Raman spectra for high-density single-walled carbon nanotube thin films. We show that the position of the main Raman mode (G) softens as the temperature increases and is nonlinear in the range of 70–270 K. This effect is explained by optical phonon decay. In the linear regime, the first-order temperature coefficient (χ_T) equals $-0.02\,cm^{-1}/K$, which is lower than for any other carbon nanotubes. Importantly, we found that local laser-induced temperature change shows a nonlinear trend as a function of global temperature with a minimum at 270 K. Our results contribute to understand the thermal properties of carbon nanotube thin films that could be applied, for example, in photovoltaic or thermoelectric devices. © *2014 AIP Publishing LLC*. [http://dx.doi.org/10.1063/1.4902522]

Since their discovery, carbon nanotubes (CNTs) have been studied intensively due to their unique opto-electronic, mechanical, and thermal properties, which allow for many applications.[1–3] Simultaneously, various CNT production methods have been extensively developed, meaning it is possible to produce supported or suspended individual carbon nanotubes[4] and more complex structures such as bundles,[5] composites with other nanoscale materials,[6] or thin films.[7] CNT thin films are more attractive than individual tubes due to their broader applicability. However, how/whether the properties of individual nanotubes change when transformed into a thin film, where nanotube interactions and topology may strongly affect the macroscopic properties, are particularly interesting because the film properties may differ significantly from those observed for an individual tube. Thus, such CNT films can be treated as a metamaterials[8] characterized by their thickness and density. Such metamaterials can be fabricated via a few methods (sprayed, aerogels, dielectrophoresis, and drop-casting)[9–12] including vacuum filtration.[7] The vacuum filtration process produces high-density films with the desired film thickness, size, and, more importantly, high homogeneity. These traits enable the use of CNT films to produce devices such as photovoltaic devices,[13] heat dissipation devices,[14] temperature sensors,[15] or optoelectronic devices.[16] For most of these applications, knowledge of the film's thermal properties is critical to their performance. Heat dissipation is currently one of the most significant performance limitations for various electronic devices. Temperature-dependent phonons behavior have been so far studied by several works dealing with individual nanotubes[4] or bundles[17–19] in high temperature range (>300 K). Nanotube rings[20] have been investigated in low temperature range showing linear and quadratic temperature dependence of phonon shifts. Up to date there has been no report on the thermal properties of thin high-density CNT films. Understanding how the thermal properties of an individual CNT change when transformed into a high-density CNT thin film, where tube-tube interfaces may strongly affect the heat and charge transfer, would be interesting because the film thermal properties may differ significantly from those observed for individual tubes.[21]

In this paper, Raman spectroscopy was used to study the thermal properties of a high-density semiconducting single-wall carbon nanotube thin film. We showed that the position of the main Raman mode (G) exhibits a nonlinear temperature dependence stemming from the optical phonon decay. Based on the obtained results, we calculated how the local thin film temperature changed with differing laser power levels. Our work may contribute to understand the thermal properties of SWCNT thin films and might be used as a starting point for determining the thermal conductivity of supported CNT thin films and the interfacial thermal resistance between a CNT thin film and the substrate.

A carbon nanotube film was produced via a vacuum filtration method and deposited onto a Si/SiO_2 substrate. In detail, carbon nanotube thin film was produced using the water solution of separated semiconducting SWCNTs from NanoIntegris (Iso-Nanotubes-S, 99% purity) with the tube diameters from 1.2 nm to 1.7 nm and the length in the range of 0.1–4 μm. The concentration of the SWCNT solution was 0.01 mg/ml. An appropriate amount of solution was vacuum filtered onto the mixed cellulose ester membrane (MCE, 0.025 μm pore-size and 25 mm diameter) to achieve specified thickness of SWCNT film. After vacuum process dry membrane with film was immersed in toluene and left overnight. Next, a 5×5 mm piece of the SWCNT film coated MCE membrane was cut and transferred face down onto Si/SiO_2 substrate (1 μm thickness of silicon dioxide). The MCE membrane was dissolved in the vapors of acetone. Finally, the sample was immersed with liquid acetone and methanol, respectively, to remove the residual MCE membrane. We note that this method allows to produce highly packed films, with an uniform thickness, and what is also important, high purity. The final result of the process is the film without residual surfactant[7] (different laser wave-length Raman measurements shown only carbon peaks). An atomic force microscope (AFM) and scanning electron microscope (SEM) were used to preliminarily characterize

a)Author to whom correspondence should be addressed. Electronic mail: zdrojek@if.pw.edu.pl. Tel./Fax: +48 22 234 7170.

the SWCNT thin films. An SEM image of the SWCNT film is shown in Fig. 1(a). The film thickness determined by the AFM measurements was approximately 40 nm (below this thickness the film loosed its uniformity).

To assess the thermal properties of the CNT films, we used a Raman scattering and temperature phonon shift technique. We chose Raman spectroscopy because it is a simple and convenient method for estimating the thermal properties of a nanomaterial. So far, this method has been applied to study the temperature effects in individual carbon nanotubes,[4] graphene,[22] WS_2,[23] and MoS_2.[24]

A schematic of the Raman experimental setup is shown in Fig. 1(b). The laser beam from the Raman spectrometer (in the backscattering configuration) was focused onto the thin film on the Si/SiO_2 substrate. A focused beam diameter on the sample of approximately 0.65 μm was calculated from the relation $2\lambda/(\pi NA)$, where λ is the laser wavelength and NA is the numerical aperture of the lens. In this setup, the laser beam plays two roles. First, it is a source of photons, which scatter inelastically during the Raman measurements; and second, it provides energy that can substantially increase the local film temperature. Thus, the Raman study enables local sample temperature increases while providing information about the temperature.

The Raman spectra were collected using a Renishaw spectrometer with a 514 nm laser (2.41 eV) excitation line to show that the main carbon G band splits into two modes denoted as G^+ and G^- (Fig. 1(c)). The stretching of the C–C bond in graphitic materials produces a so-called G-band in the Raman spectrum, which is common to all sp^2 carbon structures.[25] The curvature effects for single wall carbon nanotubes produce multiple peaks in the G-band spectrum.[25] Although up to six G-band phonons are Raman allowed for chiral SWCNTs, only two dominate the spectra: G^+ and G^-. At room temperature, the G^+ band position for an S-SWCNT thin film without any laser heating was 1593.9 cm^{-1}. In this work, the local temperature of the laser spot was estimated from the Raman G^+ line shift because its intensity is much higher than that of G^-.

To measure the temperature-dependent Raman spectra, the sample was introduced into an optical cryostat (Oxford Instrument). The temperature was varied from 70 K to 450 K with a stability of 0.1 K. The laser powers carefully calibrated on the sample were 0.05 and 7 mW. The pressure inside the chamber was approximately 10^{-6} mbar. The Raman data have been reproduced for several points in different samples with the same film thickness. No changes in the D peak have been observed confirming that no local irreversible effect in the sample morphology is seen. Also for each temperature several spectra are collected in order exclude any hysteresis effect.

Fig. 1(c) shows an example of the normalized Raman spectra for the SWCNT thin film at selected temperatures (from 70 K to 450 K) measured using the low laser power of 0.05 mW (where no laser heating is expected). More detailed results from the temperature-dependent Raman study of the G^+ mode are shown in Fig. 2, which shows a downshifted peak position and increased FWHM as a function of T. As a reminder, in this case, the peak position relates to the phonon energy ($\hbar\omega$) and FWHM corresponds to the phonon lifetime.

We used a linear approximation to analyze the Raman down shift in the G^+ peak position as a function of temperature during the first step, which uses a common formula[22]

$$\omega(T) = \omega_0 + \chi_T T, \tag{1}$$

where ω_0 is the phonon frequency at zero temperature and χ_T is the first-order temperature coefficient. The fitted slope for the lower laser power measurements is shown in Table I (the fit is presented in Fig. 2(a) using a dotted line). The χ_T coefficients for other carbon materials are also presented in Table I for comparison. Interestingly, the temperature coefficient for our thin film is lower than any individual CNTs,[26] but it seems to be higher than for CNT pellets and graphene. However, for CNT pellets,[27] the authors claim their CNT samples contained metallic particles, which may significantly lower the χ_T coefficient. Finally, this result shows that our pure CNT films exhibit a lower first-order temperature coefficient than any other CNT.

We note that purely thermal effects $(\partial\omega/\partial T)_V$ were responsible for the temperature-dependent phonon shifts in the CNTs because the volume of the related lattice expansion

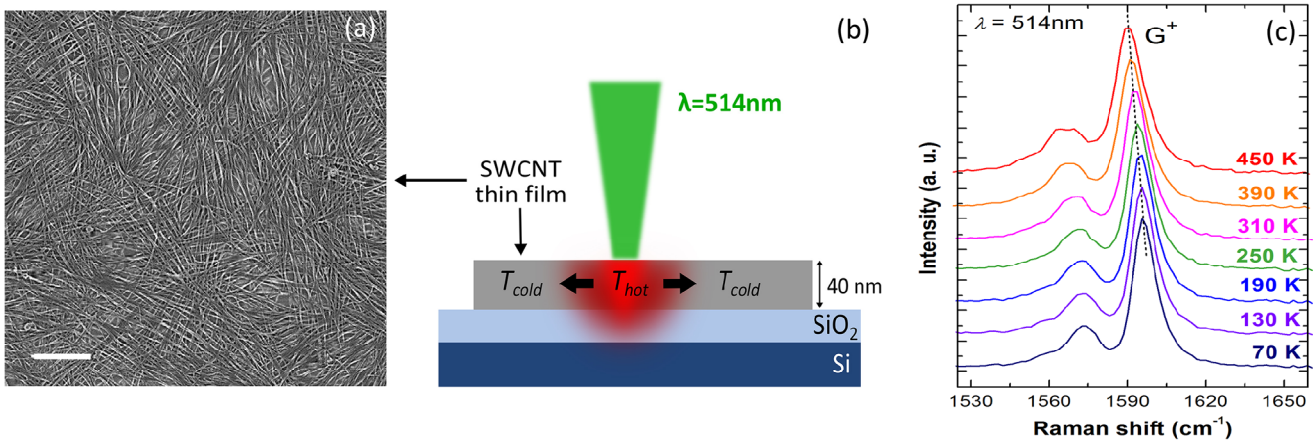

FIG. 1. (a) SEM image of a high-density single-walled CNT thin film; the scale bar represents 400 nm. (b) Schematic of the experimental setup; the focused laser spot diameter was 0.65 μm. (c) An example of normalized Raman spectra for SWCNT thin film measured at selected temperatures from 70 to 450 K using a laser power equal to 0.05 mW. The spectral resolution of the spectrometer is about 1 cm^{-1}.

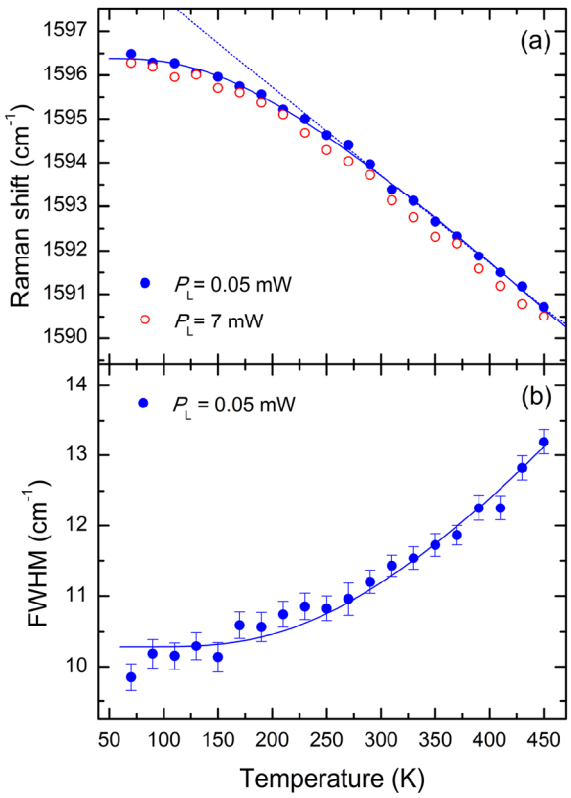

FIG. 2. (a) Temperature dependence of the Raman peak positions in the G^+ mode for SWCNT thin films using two laser powers: $P_L = 0.05$ mW (blue dots) and $P_L = 7$ mW (red open dots). The dotted line represents a fit to Eq. (1); and the solid line represents Eq. (2). The average uncertainty of determination of peak position was $<0.2\,cm^{-1}$ (error bars not shown for the sake of clarity). (b) FWHM for the G^+ mode as a function of temperature. The solid line represents the fit to Eq. (4).

effect $(\partial\omega/\partial V)_T(\partial V/\partial T)_P$ is very small (on the order of 10^{-5} 1/K)[28] and can be neglected during further analyses.

We use a second approach to describe the $\omega(T)$ dependence of the G^+ mode that is based on the formula proposed by Balkanski *et al.*[29]

$$\omega(T) = \omega_0 + A\left(1 + \frac{2}{e^x - 1}\right), \tag{2}$$

where $x = \hbar(\omega_0/2)/k_B T$, $\hbar$ is Planck's constant, k_B is the Boltzmann constant, A is the fitting parameter, and T is the sample temperature without laser heating ($P_L = 0.05$ mW). This model describes the effect optical phonon decay has on two acoustic phonons with equal energies due to potential anharmonicity in the structure. This approximation was represented by the solid lines in Fig. 2(a). The values of fit parameters: ω_0 and A are shown in Table I. We found that this relation better described the experimental G^+ peak (LO phonons) position data as a function of temperature than Eq. (1), especially in the lower temperature range (<270 K). Interestingly, the nonlinear behavior shown here for SWCNT thin films was also observed for single-layer materials: MoS_2,[24] WS_2,[23] and most importantly, suspended single wall carbon nanotubes obtained via chemical vapor deposition[4] or supported SWCNTs[19] (where this effect was related to contributions from electron-phonon interactions).

For higher temperatures, formula (2) turns into a linear dependency because $x = \frac{\hbar(\omega_0)}{2k_B T} \ll 1$

$$\omega(T) \overset{x\ll 1}{\rightarrow} \omega_0 + A + \frac{4Ak_B}{\hbar\omega_0}T = \omega_0' + \chi_B T, \tag{3}$$

where $\omega_0' = \omega_0 + A$ and $\chi_B = \frac{4Ak_B}{\hbar\omega_0}T$; therefore, the theoretical functions (1) and (2) converge.

Figure 2(b) shows the experimental Raman peak width (FWHM) data as a function of temperature for both laser powers. We fit the experimental data to the three-phonon process described by the following equation:[29]

$$\Gamma(T) = \Gamma_0\left(1 + \frac{2}{e^x - 1}\right), \tag{4}$$

where Γ_0 is the peak width at zero temperature. The theoretical curve fit the data quite well, which confirms that the phonon decay process is responsible for the nonlinear temperature-dependent behavior of $\Gamma(T)$. The fit parameters are detailed in Table I. These results are in good agreement with studies of phonon population dynamics in nanotube bundles probed by time-resolved Raman spectroscopy.[30,31] These works, however, do not show the corresponding change in the phonon energies.

In theory, the FWHM could also serve as a local thermometer. However, in this work, we used the peak position as the temperature indicator because the uncertainties when estimating the peak position were lower than those for the FWHM.

To describe how the laser power level changes the local SWCNT thin film temperature, we measured two Raman spectra at each temperature using $P_L = 0.05$ mW and $P_L = 7$ mW, where P_L is the laser power on the sample. At the higher laser power, the Raman peaks downshift due to the local heating (see the hollow circles in Fig. 2(a)).

TABLE I. Calculated parameters from Eqs. (1), (2), and (4) for the lower laser power data and comparisons with the literature. Symbols a and b correspond to the different temperature regimes.

Sample	χ_T (cm^{-1}/K) Eq. (1)	ω_0 (cm^{-1}) Eq. (1)	ω_0 (cm^{-1}) Eq. (2)	A (cm^{-1}) Eq. (2)	Γ_0 (cm^{-1}) Eq. (4)	Temperature range (K)
This work	−0.0201[a]	1599.7[a]	1602.5[b]	−6.16[b]	10.29[b]	270–450[a]/70–450[b]
Suspended SWCNT[26]	−0.03321	1587.14	…	…	…	183–363
SWCNT + catalysts pellet[27]	−0.0189	1599.1	…	…	…	299–773
SWCNT bundles[32]	−0.0407	1591.2	…	…	…	300–673
DWCNT[33]	…	…	1596	−11	…	80–700
DWCNT[34]	−0.022	…	…	…	…	175–320
MWCNT[35]	−0.023	…	…	…	…	320–840
Supported graphene[22]	−0.016	1584	…	…	…	83–373

An example of the different G^+ peak positions between the two laser powers for T = 350 K (the temperature inside the cryostat) is shown in Fig. 3(a). The negative $\Delta\omega$ reflects the phonon downshift with increasing temperature. The measured $\Delta\omega$ results across the full temperature range are shown in Fig. 3(b). The peak position dependence is a monotonic function of the temperature with a calculated slope of $-0.007\,cm^{-1}/K$.

The temperature increase due to the increased laser power was calculated in the following way. Using a fixed global temperature (temperature for the cryostat and entire sample without laser heating), we measured the temperature corresponding to the G^+ peak position for two laser powers. For this purpose, we used the data calculated from Balkanski's equation for the lower laser power measurements as shown in Fig. 2(a) with the data presented in Fig. 3(a). The obtained temperature differences for both series (collected using the lower and higher laser power) were the local temperature change and are presented in Fig. 3(b). We note that the local temperature decreased slightly as the global temperature increases to 270 K. Below 270 K, the local temperature began to increase. This result indicates the most effective heat dissipation in our thin film occurred at T = 270 K and most likely suggests a nonlinear thermal conductivity (κ) behavior for the thin film as a function of temperature. Another, however less possible, explanation for this nonlinear effect could be a change in the interfacial thermal resistance with temperature, for example, by freezing the phonons at the film-SiO_2 interface. Further, study is needed to clarify this effect.

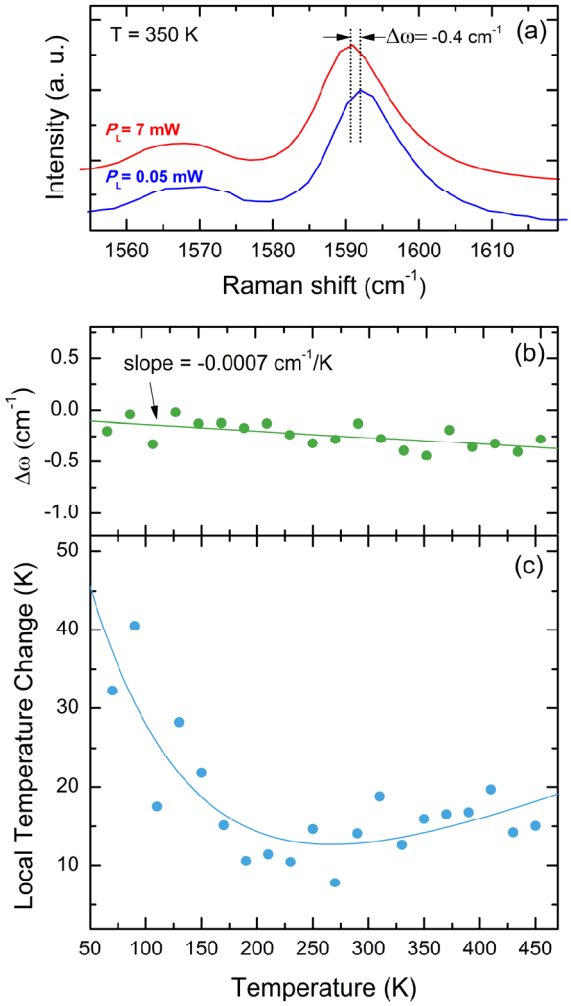

FIG. 3. (a) Raman spectra of the SWCNT thin film for both laser powers taken at 350 K. We note the small difference between peaks position ($0.4\,cm^{-1}$) are determined from the fit of the measured data. (b) Change in the G^+ peak position due to the absorbed laser power at different temperatures. The line represents a linear fit. (c) Calculated local temperature change. The curve is only a guide for the eye.

In conclusion, we experimentally investigated the temperature-dependent Raman spectra for a semiconducting SWCNT thin film at temperatures from 70 K to 450 K and demonstrated the softening of the main Raman mode position (G^+) with increasing temperature. We found that the phonon shifts in the G^+ mode below 270 K exhibit a nonlinear dependence on the global temperature. The temperature coefficient calculated using the lower laser power (0.05 mW) was $-0.201\,cm^{-1}/K$. We concluded that the obtained effects stem from optical phonon decay due to the potential anharmonicity in the SWCNT thin film structure. Local temperature changes in the supported semiconducting SWCNT thin film under laser heating were calculated from the Raman measurements as a function of the global temperature. We found that the local temperature characteristic had a minimum at 270 K. We claim the observed effect might relate to changes in the thermal conductivity or thermal interface resistance as a function of the SWCNT thin film temperature, and more work is needed to clarify this effect. Our results maybe useful for future studies on the thermal properties of carbon nanotube thin films.

The work was supported by the Lider project founded by NCBR (Lider/11/22/L-2/10/NCBR/2011). A.D. was also supported by the European Union via the European Social Fund through the Warsaw University of Technology Development Program.

[1]M. F. L. De Volder, S. H. Tawfick, R. H. Baughman, and A. J. Hart, Science **339**, 535 (2013).
[2]M. Scarselli, P. Castrucci, and M. De Crescenzi, J. Phys.: Condens. Matter **24**, 313202 (2012).
[3]S. Park, M. Vosguerichian, and Z. Bao, Nanoscale **5**, 1727 (2013).
[4]X. Zhang, F. Yang, D. Zhao, L. Cai, P. Luan, Q. Zhang, W. Zhou, N. Zhang, Q. Fan, Y. Wang, H. Liu, W. Zhou, and S. Xie, Nanoscale **6**, 3949 (2014).
[5]P. Gowda, A. Suri, S. K. Reddy, and A. Misra, Nanotechnology **25**, 025708 (2014).
[6]S. Hrapovic, E. Majid, Y. Liu, K. Male, and H. T. Luong, Anal. Chem. **78**, 5504 (2006).
[7]Z. Wu, Z. Chen, X. Du, J. M. Logan, J. Sippel, M. Nikolou, K. Kamaras, J. R. Reynolds, D. B. Tanner, A. F. Hebard, and A. G. Rinzler, Science **305**, 1273 (2004).
[8]J. T. Hong, D. J. Park, J. H. Yim, J. K. Park, J. Y. Park, S. Lee, and Y. H. Ahn, J. Phys. Chem. Lett. **4**, 3950 (2013).
[9]Z. Li, V. P. Kunets, V. Saini, Y. Xu, E. Dervishi, G. J. Salamo, A. R. Biris, and A. S. Biris, ACS Nano **3**, 1407 (2009).
[10]K. J. Zhang, A. Yadav, K. H. Kim, Y. Oh, F. Islam, C. Uher, and K. P. Pipe, Adv. Mater. **25**, 2926 (2013).
[11]S. Shekhar, H. Heinrich, and S. I. Khondaker, Carbon **50**, 1635 (2012).
[12]M. Grechko, Y. Ye, R. D. Mehlenbacher, T. J. McDonough, M. Y. Wu, R. M. Jacobberger, M. S. Arnold, and M. T. Zanni, ACS Nano **8**, 5383 (2014).
[13]V. L. Borgne, L. A. Gautier, P. Castrucci, S. Del Gobbo, M. De Crescenzi, and M. A. El Khakani, Nanotechnology **23**, 215206 (2012).

[14]S. Jiang, C. Liu, and S. Fan, ACS Appl. Mater. Interfaces **6**, 3075 (2014).
[15]A. Di Bartolomeo, M. Sarno, F. Giubileo, C. Altavilla, L. Iemmo, S. Piano, F. Bobba, M. Longobardi, A. Scarfato, D. Sannino, A. M. Cucolo, and P. Ciambelli, J. Appl. Phys. **105**, 064518 (2009).
[16]A. Behnam, J. Johnson, Y. Choi, L. Noriega, M. G. Ertosun, Z. Wu, A. G. Rinzler, P. Kapur, K. C. Saraswat, and A. Ural, J. Appl. Phys. **103**, 114315 (2008).
[17]A. N. Volkov, R. N. Salaway, and L. V. Zhigilei, J. Appl. Phys. **114**, 104301 (2013).
[18]H. D. Li, K. T. Yue, Z. L. Lian, Y. Zhan, L. X. Zhou, S. L. Zhang, Z. J. Shi, Z. N. Gu, B. B. Liu, R. S. Yang, H. B. Yang, G. T. Zou, Y. Zhang, and S. Iijima, Appl. Phys. Lett. **76**, 2053 (2000).
[19]S. Chiashi, Y. Murakami, Y. Miyauchi, and S. Maruyama, Jpn. J. Appl. Phys., Part 1 **47**, 2010 (2008).
[20]L. Song, W. Ma, Y. Ren, W. Zhou, S. Xie, P. Tan, and L. Sun, Appl. Phys. Lett. **92**, 121905 (2008).
[21]A. A. Balandin, Nat. Mater. **10**, 569 (2011).
[22]I. Calizo, A. A. Balandin, W. Bao, F. Miao, and C. N. Lau, Nano Lett. **7**, 2645 (2007).
[23]M. Thripuranthaka and J. L. Dattatray, ACS Appl. Mater. Interfaces **6**, 1158 (2014).
[24]A. Taube, J. Judek, C. Jastrzębski, A. Duzynska, K. Świtkowski, and M. Zdrojek, ACS Appl. Mater. Interfaces **6**, 8959 (2014).
[25]M. S. Dresselhaus, G. Dresselhaus, R. Saito, and A. Jorio, Phys. Rep. **409**, 47 (2005).
[26]H. D. Wang, J. H. Liu, Z. Y. Guo, X. Zhang, R. F. Zhang, F. Wei, and T. Y. Li, Nanoscale Microscale Thermophys. Eng. **17**, 349 (2013).
[27]N. R. Raravikar, P. Keblinski, A. M. Rao, M. S. Dresselhaus, L. S. Schadler, and P. M. Ajayan, Phys. Rev. B **66**, 235424 (2002).
[28]Y. Maniwa, R. Fujiwara, H. Kira, H. Tou, H. Katura, S. Suzuki, Y. Achiba, E. Nishibori, M. Takata, M. Sakata, A. Fujiwara, and H. Suematsu, Phys. Rev. B **64**, 241402(R) (2001).
[29]M. Balkanski, R. F. Wallis, and E. Haro, Phys. Rev. B **28**, 1928 (1983).
[30]J. Nesbitt and D. C. Smith, Phys. Rev. B **87**, 195446 (2013).
[31]I. Chatzakis, H. Yan, D. Song, S. Berciaud, and T. Heinz, Phys. Rev. B **83**, 205411 (2011).
[32]Q. Zhang, D. J. Yang, S. G. Wang, S. F. Yoon, and J. Ahn, Smart Mater. Struct. **15**, S1 (2006).
[33]M. Sendova, E. Flahaut, and T. Hartsfield, J. Appl. Phys. **108**, 044309 (2010).
[34]A. Bassil, P. Puech, L. Tubery, and W. Bacsa, Appl. Phys. Lett. **88**, 173113 (2006).
[35]F. Huang, K. T. Yue, P. Tan, S. L. Zhang, Z. Shi, X. Zhou, and Z. Gu, J. Appl. Phys. **84**, 4022 (1998).